Soft Matter

PAPER

View Article Online
View Journal | View Issue

Open Access Article. Published on 12 June 2015. Downloaded on 12/5/2025 12:04:56 PM.
This article is licensed under a Creative Commons Attribution 3.0 Unported Licence.

Cite this: *Soft Matter*, 2015, **11**, 5554

Fractional Debye–Stokes–Einstein behaviour in an ultraviscous nanocolloid: glycerol and silver nanoparticles

Szymon Starzonek,[ab] Sylwester J. Rzoska,*[ab] A. Drozd-Rzoska,[b] Sebastian Pawlus,[a] Ewelina Biała,[a] Julio Cesar Martinez-Garcia[c] and Ludmila Kistersky[d]

Received 1st February 2015,
Accepted 22nd May 2015

DOI: 10.1039/c5sm00266d

www.rsc.org/softmatter

One of the major features of glass forming ultraviscous liquids is the decoupling between translational and orientational dynamics. This paper presents studies of this phenomenon in glycerol, an accepted molecular glass former, concentrating on the impact of two exogenic factors: high pressures (P) up to the extreme 1.5 GPa and silver (Ag) nanoparticles (NPs). The analysis is focused on the fractional Debye–Stokes–Einstein (FDSE) relationship: $\sigma(T,P)(\tau(T,P))^S$ = const, linking DC electric conductivity (σ) and primary (alpha, structural) relaxation time (τ_α). In glycerol and its nanocolloid (glycerol + Ag NPs) at atmospheric pressure only negligible decoupling ($S \sim 1$) was detected. However, in the compressed nanocolloid, a well-defined transformation (at P = 1.2 GPa) from $S \sim 1$ to the very strongly decoupled dynamics ($S \sim 0.5$) occurred. For comparison, in pressurized 'pure' glycerol the stretched shift from $S \sim 1$ to $S \sim 0.7$ took place. This paper also presents the general discussion of FDSE behavior in ultraviscous liquids, including the new link between the FDSE exponent, fragility and the apparent activation enthalpy and volume.

Introduction

Glass transition physics has remained a challenge for condensed and soft matter physics for many decades.[1–3] The most intriguing feature is the set of strong previtreous effects for dynamic properties, with similar patterns for qualitatively different glass forming systems.[2] The key representative of such behavior is the super-Arrhenius (SA) evolution of various dynamic properties on approaching the glass temperature (T_g):[2,3]

$$x(T) = x_0 \exp\left(\frac{\Delta E_a(T)}{RT}\right), \quad T > T_g \qquad (1)$$

where $x(T)$ is the primary (structural, alpha) relaxation time (τ_α), viscosity (η), diffusion (D) or reciprocal of direct current (DC) electric conductivity ($1/\sigma$). $\Delta E_a(T)$ denotes the apparent activation energy, T_g is the glass transition temperature and R is the gas constant.

The basic Arrhenius equation can be restored for $\Delta E_a(T) = \Delta E_a$ = const.

[a] *Silesian Intercollegiate Center for Education and Interdisciplinary Research & Institute of Physics, University of Silesia, ul. 75 Pułku Piechoty 1A, 41-500 Chorzów, Poland. E-mail: sylwester.rzoska@gmail.com*
[b] *Institute of High Pressure Physics, Polish Academy of Sciences, ul. Sokołowska 27/39, 01-142 Warsaw, Poland*
[c] *University of Bern, Freiestrasse 3, Bern CH-3012, Switzerland*
[d] *V. Bakul Institute for Superhard Materials of the National Academy of Superhard materials NASU, Avtozavodskaya Str.2, 04074 Kiev, Ukraine*

The 'universal' metric of the SA behavior is called 'fragility' and is defined as:[2,4]

$$m = m_{P=\text{const}} = \left[\frac{\mathrm{d}\log_{10} x(T)}{\mathrm{d}(T/T_g)}\right]_{T=T_g} \qquad (2)$$

It ranges from $m \approx 16$ for the 'clear' Arrhenius behavior to $m \sim 200$ for the strongly SA dynamics. The fragility is considered to be one of the most important parameters of glass transition physics: the metric linking microscopically distinct systems, including low molecular weight liquids (LMW), polymers, colloids and so on.[2,5] Nevertheless, its fundamental meaning is still well characterized by the title of ref. 6: 'The fragility and other properties of glass-forming liquids: Two decades of puzzling correlations''. Only recently, a clear link to basic process energies was derived:[5] $m = C(\Delta H_a/\Delta E_a)_{T=T_g}$, where $C = \log\tau_\alpha(T_g) - \log\tau_0$, $\Delta H_a = \mathrm{d}\ln\tau_\alpha(T_g)/\mathrm{d}(1/T_g)$ is the activation enthalpy, $\tau_\alpha(T_g)$ = 100 s and $\tau_0 = 10^{-11}$–10^{-16} s is the prefactor in the SA eqn (1). The SA behavior is assisted by the stretched exponential (SE) time decay of the physical properties: $I(t) \propto \exp[-(t/\tau_\alpha)^\beta]$, with the SE exponent $0 < \beta \leq 1$ or equivalently the non-Debye distribution of relaxation times in the frequency domain.[2]

It is particularly notable that the evolution of translation and orientation related dynamic properties ($x(T)$) in the ultraviscous domain near T_g is decoupled, which is manifested by the fractional Stokes–Einstein (FSE) and fractional Debye–Stokes–Einstein (FDSE) relationships:[2,7–10]

This journal is © The Royal Society of Chemistry 2015

Open Access Article. Published on 12 June 2015. Downloaded on 12/5/2025 12:04:56 PM.
This article is licensed under a Creative Commons Attribution 3.0 Unported Licence.

$D/T = A\eta^{-1+\varpi}$ and $D/T = A'\tau_\alpha^{-1+\varpi}$ with the exponent $\varsigma = 1 - \varpi$ (3)

$$\sigma\tau_\alpha^{1-\mu} = \text{const} \quad \text{with the exponent } S = 1 - \mu \tag{4}$$

where A and A' are constants.

The experimental evidence indicates that generally FDSE or FSE behavior with non-zero fractional exponents (ϖ,$\mu \neq 0$) takes place in the ultraviscous/ultraslowing dynamical domain for T_B ($\tau_\alpha \sim 10^{-7}$ s, $\eta \sim 10^3$ Poise) $< T(\tau,\eta) < T_g$ ($\tau_\alpha \sim 10^2$ s, $\eta \sim 10^{13}$ Poise). For $T > T_B$ the crossover to Debye–Stokes–Einstein (DSE) or SE behavior occurs when (ϖ,$\mu = 0$ or ζ,$S = 1$).[2,8–40] The temperature T_B is related to the crossover from the high temperature (ergodic) to the low-temperature (non-ergodic) dynamic domain.[2,11] The latter is also associated with the appearance of multimolecular dynamic heterogeneities (DHs) or alternatively cooperatively rearranging regions near the T_g, with vastly different relaxation times and viscosity.[2,16–40] They are considered as the most probable reason for the universal patterns in the ultraviscous/ultraslowing (low temperature) domain in the immediate vicinity of the T_g.[2] Studies of FDSE or FSE behavior are recognized as one of key tools for obtaining insight into, the still mysterious, dynamic heterogeneities.[2,8,15] Nevertheless, the knowledge regarding the fundamental background of FDSE/FSE behavior is still heuristic, despite the growing number of experimental and theoretical research reports.[2,7–40]

All these suggests the significance of FDSE studies in ultraviscous liquids atemporal 'research status quo'. This is the target of this report.

Firstly, an outline of the FDSE reference results will be given, particularly focusing on eqn (4), is presented. This topic is concluded by exploring the novel link between the FDSE exponent and the basic characteristics of the SA behavior, namely: the fragility, the activation enthalpy and the activation volume. Secondly, results related to the impact of exogenic factors on the dynamics of glycerol, one of the accepted glass forming liquids, are presented. They are: (i) high pressures up to a challenging $P = 1.5$ GPa and (ii) the addition of silver nanoparticles (Ag NP), forming a nanocolloid/nanocomposite/nanofluid with the ultraviscous glycerol. The impact of NPs lead to the crossover of the strongly decoupled region in the immediate vicinity of the T_g, *i.e.*, within the ultraviscous domain, a phenomenon which has not been reported before.

II. The translational–orientational decoupling

For coupling between translational and orientational processes in 'classical' liquids one can expect the Debye, Stokes and Einstein relationships to be valid:[2,14,41]

$$\frac{D_{tr}}{T} = \frac{k_B}{6\pi r_{ion}}\eta^{-1}, \tag{5}$$

$$\tau_\alpha = \frac{\nu\eta}{k_B T}, \tag{6}$$

$$\frac{D_{rot}}{T} = \frac{k_B}{8\pi {r_{dip}}^3}\eta^{-1} \tag{7}$$

where D_{tr} and D_{rot} denote translational and rotational diffusivities, $\nu = A'V$, r is the radius of the diffusing molecule and V is the molecular volume.

It is notable that for the Debye–Stokes (DS) equation [eqn (6)], $\tau_\alpha(T) \propto \eta(T)/T$.[15,41] However, the alternative approach by the Maxwell relationship[15] gives $\tau = G_\infty\eta$. Consequently, assuming that in the ultraviscous domain the instantaneous shear modulus G_∞ = const one obtains $\tau(T) \propto \eta(T)$.[15] It is worth recalling that in the Maxwell relationship, τ denotes the stress relaxation time and there is no clear experimental evidence that the structural (τ_α) and stress relaxation time (τ) are interchangeable.[2,15] Linking the above dependences with the Nernst–Einstein (NE) relationship $D_{tr} = k_B T\sigma/nq^2$,[14] where n is the number of electric charges/carriers, σ denotes the DC electric conductivity and q is the electric charge, one obtains:

$$\sigma\tau_\alpha = \frac{nq^2 C\nu}{k_B T}, \ i.e., \ T\sigma\tau_\alpha = \text{const} \tag{8}$$

or

$$\sigma\tau_\alpha = \frac{CG_\infty ne^2}{a}, \ i.e., \ \sigma\tau_\alpha \approx \text{const} \tag{9}$$

where eqn (8) recalls the DS eqn (5) and (9) is based on the Maxwell equation, as discussed previously.

In low molecular weight liquids the DC conductivity arises from residual ionic dopants: salts or other ionic species that inevitably get into samples during their synthesis.[12] For broad band dielectric spectra (BDS) such behavior always dominates at lower frequencies, often beginning just below the kHz domain. In ionic or highly conductive liquids this can also be the governing factor for the multi MHz region. It is notable that taking into account the Nernst–Smoluchowski relationship (NS: $D_{tr} = \lambda/2\tau_h$),[14,41,42] and the NE equations one obtains the relationship linking DC conductivity and the hopping time of ions, responsible for the DC conductivity, namely:

$$\sigma = \frac{nq^2}{kT}\frac{\lambda}{2\tau_h} \tag{10}$$

where τ_h is the hopping length of the diffusing species, n is the concentration of free ions and q is the ion charge.

This relationship makes it possible to present eqn (3)–(7) as the result of the comparison between the two time scales associated with the orientation of molecules (~primary, alpha, structural relaxation) and the translation related ions hopping time. The entrance into the ultraviscous domain converts eqn (10), NS and NE relationships into their fractional forms. Consequently, FSE and FDSE eqn (3) and (4) can be presented as the results of the comparison of the two previously mentioned timescales:[43]

$$\frac{\tau_\alpha}{\tau_h} \propto (\tau_\alpha)^\mu \quad \text{and} \quad \frac{\tau_\alpha}{\tau_h} \propto (\tau_\alpha)^\varpi \tag{11}$$

which suggests that $1/\tau_h \propto \sigma$ and the exponents $\mu = \varpi$.

The last dependence resembles the one used in polymeric systems for the comparison of segmental (τ_S) and chain (τ_C) relaxation processes: $R = \tau_S/\tau_C \propto (\tau_S)^\varepsilon$. For LMW liquids, the

Open Access Article. Published on 12 June 2015. Downloaded on 12/5/2025 12:04:56 PM.
This article is licensed under a Creative Commons Attribution 3.0 Unported Licence.

primary relaxation time τ_α can be compared to τ_S and τ_C on the large time scale: in polymers it is estimated by $\tau_C \propto \langle\tau_S\rangle$. In ref. 43 the thermally activated barrier hopping model for the glass transition phenomenon is recalled to enable a deeper discussion of this issue. This model assumes that the leading role of heterogeneities/(local domains) is coordinating a group of molecules (LMW) or segments (P) in the ultraviscous/ultra-slowing region. Fluctuating local density excesses result in a distribution of barrier heights, which gives rise to the decoupling of primary relaxation time and diffusion related processes as well as to the stretched exponential (non-Debye) relaxation. For polymers this 'heterogeneous' model yields: $\varepsilon = \Delta/(1+\Delta) = 1 + (1/a_c q)$, where $\Delta = a_C q' = a_C \sigma_E^2/2\langle F_B\rangle$, σ_E^2 is the energy barrier fluctuations variance, $\Delta E_a(T) = a_c F_B(T)$ in SA eqn (1), a_c is a presumably temperature independent cooperation parameter, $F_B(T)$ is the hopping barrier energy and $\langle F_B(T)\rangle$ is the mean value. The parameter $q' = 0.1$–0.2 is the volume fraction of cooperative domains (heterogeneities). Based on the previous dependences and the semi-empirical correlation for the fragility $m = 16 + 40.6(a_c)^{0.56}$ in polymers, one can directly arrive at the relationship which can easily be tested experimentally:[43]

$$\frac{1}{\varepsilon} = \frac{q'}{[(m-16)/40.6]^{0.56}} \qquad (12)$$

The compilation of experimental data for polymeric glass formers confirmed the smooth dependence of ε versus fragility m predicted by the above relationship. The important result of ref. 43 was that the chain relaxation and fragility should depend weakly on the material as well as be insensitive to local heterogeneities because of the large scale averaged nature of τ_C. This behavior is in strong contrast to 'segmental' related dynamics (τ_S), where there are notably SA behavior and fragility (large m values). All these can be associated with local cooperativeness ('heterogeneities'). Sokolov and Schweitzer[43] suggested the same scenario for non-polymeric ultraviscous liquids, which leads to the equivalence: $\tau_C \rightarrow \tau_h(\propto 1/\sigma, 1/D_{tr})$ and $\tau_S \rightarrow \tau_\alpha$ in polymers and LMW, respectively. It is notable that the link of fractional decoupling exponents to DHs is the output result of various glass transition models.[43] However, eqn (12) offers a unique possibility of experimental tests of such hypothesis. Nevertheless, it is also associated with a notable arbitrariness, namely: (i) it includes the assumption that the prefactor in eqn (1) is universal ($\tau_0 = 10^{-14}$ s and then $C = 16$), (ii) the average energy $\langle F_B\rangle$ is poorly defined because of strong changes within the ultraviscous domain and for different glass formers.

In experimental studies on ultraviscous LMW liquids, particular attention was paid to eqn (4) linking structural relaxation time and DC electric conductivity. So far, this is the only 'fractional coupling' relationship which can be tested both as the function of temperature and pressure. Furthermore, experimental values of $\sigma(T,P)$ and $\tau_\alpha(T,P)$ can be determined from the same scan of the imaginary part of dielectric permittivity $\varepsilon''(f)$, using the BDS. This fact essentially reduces biasing artifacts. There is broad experimental evidence supporting the validity of FDSE eqn (4), (8) and (9) and showing that the exponent $0.75 < S < 0.9$.[2,10,16–26,37–41] Psurek *et al.*[20,23,24] indicated a possible pressure–temperature isomorphism for the FDSE behavior, namely:

$$\sigma(T,P)\tau_\alpha(T,P)^{1-\mu} = \text{const}, \quad 1-\mu = S \qquad (13)$$

It is notable that the pressure studies focused on testing eqn (13) were carried out for relaxation times 10^{-6} s $< \tau_\alpha <$ (10^{-1}–10^{-3} s) for near room temperatures and moderate pressures $P < 0.3$ GPa.[2,10,16–26,37–41] Such limitations resulted from frequency restrictions still existing in high pressure BDS studies.[13] Nevertheless, the tested time scale in pressure studies was well located within the ultraviscous and low temperature domain, adjusting to the glass transition at (P_g,T_g).[2,11]

When discussing the FDSE behavior in glass forming ultraviscous liquids, it is worth recalling that the challenging compilation of experimental data for 50 glass forming liquids focused on the normalized version of the FDSE eqn (4).[8] For all liquids in the ultraviscous domain the same 'universal' FDSE exponent $\zeta \approx 0.85$, *i.e.* $\omega \approx 0.15$ was obtained.[8] This analysis included glycerol, which is the object of this paper. It is notable that linking eqn (3), (4) and (8), one obtains:

$$\sigma\tau_\alpha^\zeta = \frac{CG_\infty^{-\zeta} nq^2}{a}, \ \textit{i.e.}, \ \text{the fraction exponent } S = \zeta \qquad (14)$$

This result suggests the hypothetical equivalence of all the previously discussed FDSE power exponents. Although the vast majority of experimental evidence supports the appearance of FDSE behavior in ultraviscous glass formers, or even more generally in highly viscous soft matter–complex liquids systems, results indicating a gradual decrease of FDSE exponents also exist. It is also worth recalling that there are controversies related to the question of whether the FDSE behavior is described by $T\sigma\tau_\alpha^S \approx$ const[2,15] or $\sigma\tau_\alpha^S \approx$ const.[2,13–40] The prevalence of the evidence supporting the latter dependence is most often explained by the statement that in the tested range of temperatures in ultraviscous liquids the change of temperature is small and negligible.[13,16–18] In the opinion of the authors of this paper, this 'general claim' poorly coincides with the fact that the ultraviscous domain extends up to even $\Delta T \approx 100$ K. Regarding this fundamental issue, the discussion related to eqn (8) and (9) indicates that the dependence $\sigma\tau_\alpha^S \approx$ const is related to the 'elastic' Maxwell model with G_∞ = const, and such behavior seems to dominate in the ultraviscous domain. One can expect that the inherent features of the Debye model are responsible for the fact that the relationship $T\sigma\tau_\alpha^S \approx$ const may be valid in the high temperature domain.

Generally the pressure counterpart of the SA eqn (1) is given by:[2,13,42]

$$x(P) = x_0^P \exp\left(\frac{P\Delta V_a^x(P)}{RT}\right), \quad T = \text{const.} \qquad (15)$$

where $\Delta V_a(P)$ is the apparent activation volume ('free volume').

It can be called super-Barus (SB), because the basic equation proposed by Barus[44] $x(P) = x_0^P \exp(cP)$ can be rewritten as $\Delta V_a^x/RT = c$ = const. The SA eqn (1) enables the determination of the apparent activation enthalpy using $\Delta H_a^x(T)/R = \mathrm{d}\ln x(T)/\mathrm{d}(1/T)$.[45–47]

 This journal is © The Royal Society of Chemistry 2015

Open Access Article. Published on 12 June 2015. Downloaded on 12/5/2025 12:04:56 PM.
This article is licensed under a Creative Commons Attribution 3.0 Unported Licence.

Following ref. 2 and 45–47 the SB eqn (15) gives the apparent activation volume by $\Delta V_a^x(T)/R = \mathrm{d}\ln x(T)/\mathrm{d}(1/T)$. Then, based on the FDSE eqn (13) one obtains:

$$\begin{cases} -\dfrac{\mathrm{d}\ln\sigma(P)}{\mathrm{d}P} + S\dfrac{\mathrm{d}\ln\tau_\alpha(T)}{\mathrm{d}P} = -\dfrac{\Delta V_a^\sigma(P)}{RT} + S\dfrac{\Delta V_a^\tau(P)}{RT} = 0 \\ \Rightarrow S = \dfrac{\Delta V_a^\sigma}{\Delta V_a^\tau} \\ -\dfrac{\mathrm{d}\ln\sigma(T)}{\mathrm{d}(1/T)} + S\dfrac{\mathrm{d}\ln\tau_\alpha(T)}{\mathrm{d}(1/T)} = -\dfrac{\Delta H_a^\sigma(T)}{RT} + S\dfrac{\Delta H_a^\tau(T)}{RT} = 0 \\ \Rightarrow S = \dfrac{\Delta H_a^\sigma}{\Delta H_a^\tau} \end{cases} \quad (16)$$

Consequently, for a given point in the (P,T) plane:

$$S = \frac{\Delta H_a^\sigma}{\Delta H_a^\tau} = \frac{\Delta V_a^\sigma}{\Delta V_a^\tau} \quad (17)$$

Direct implementations of the SA eqn (1) or the SB eqn (15) for portraying experimental data are not possible, because of the unknown forms of the apparent activation energy and volume. Consequently, ersatz dependences are used. The dominant is the Vogel–Fulcher–Tammann (VFT) relationship[2,12] or its pressure related quasi-counterpart introduced in ref. 48:

$$x(T) = x_0^T \exp\left(\frac{D_T T_0}{T - T_0}\right) \quad (18)$$

$$x(P) = x_0^P \exp\left(\frac{D_P P_0}{P_0 - P}\right) \quad (19)$$

where (T_0,P_0) are VFT singular temperature and pressures, located in the solid glass phase. D_T, D_P are fragility strength coefficients related to the temperature of the pressure path of the approaching the glass transition.

Despite the success of the VFT equation in empirical applications and model analysis,[2–4,12,13] its general fundamental validity has been questioned recently.[5,46,47] However, glycerol can be encountered in the limited group of materials where the VFT parameterization remains valid.[47] With the SA and SB behavior inherently associated with the concept of fragility, it is one of the most prominent ideas within the glass transition physics field.[2,4,12,13] The fragility constitutes the metrics of the 'degree' of the SA or SB behavior over basic Arrhenius or Barus ones. It is defined by the temperature related isobaric fragility (eqn (2)) and for the isothermic, pressure related path as: $m_{T=\mathrm{const}} = [\mathrm{d}\log_{10} x(P)/\mathrm{d}(P/P_g)]_{P=P_g}$.[13,45,48,49]

In ref. 45 following the links between $x(T,P)$, experimental data and basic parameters describing SA or SA dynamics were derived:

$$\mathrm{d}\ln x(T)/\mathrm{d}(1/T) = \Delta H_a^x/R = Tm_p/\log_{10} e \text{ for } P = \text{const} \quad (20)$$

and

$$\mathrm{d}\ln x(P)/\mathrm{d}P = \Delta V_a^x/RT = m_T/\log_{10} e \text{ for } T = \text{const}. \quad (21)$$

Their substitution into eqn (13) gives the link between fragility and the FDSE exponent:

$$\begin{aligned} S &= \frac{\Delta H_a^\sigma}{\Delta H_a^\tau} = \frac{\mathrm{m}_P^\sigma}{m_P^\tau}\,(P = \text{const}) \quad \text{and} \\ S &= \frac{\Delta V_a^\sigma}{\Delta V_a^\tau} = \frac{m_T^\sigma}{m_T^\tau}\,(T = \text{const}) \end{aligned} \quad (22)$$

Experimental

A fluid nanocomposite–nanocolloidal mixture with the concentration reaching 180 ppm of Ag NPs in glycerol was prepared at the Institute of Superhard Materials in Kiev, Ukraine. It is notable that no additional chemicals or surfactants were needed to stabilize the nanocolloid and to avoid the sedimentation. Ag NP were synthesized using the localized ion-plasma sputtering and immediate implantation of freshly created NPs to the carrier liquid in vacuum which allows highly concentrated stable dispersions of ultra clean metal nanoparticles in various carrier liquids to be produced.[50] The size distribution of the NPs, averaged at ~25 nm was below 2%, which is shown in Fig. 1. The concentration of Ag NP (180 ppm) was the highest for which long-term stability (at least one year) was reached, without the addition of any other component. However, a further increase of NP concentration led to their aggregation. Fig. 1 also contains two photographs: (i) the bottle with the nanocolloid and (ii) the scanning electron microscopy (SEM) image (ambient conditions). For the latter, the view was influenced by the preparation for the SEM treatment and the fact that several layers of Ag NPs are 'collected' on a plate.

The quality of NPs was comparable with the ultraclean solutions produced by laser ablation in liquids but the combined ion plasma sputtering demonstrated much higher productivity and cost effectiveness.[50,51] Nevertheless, immediately prior to

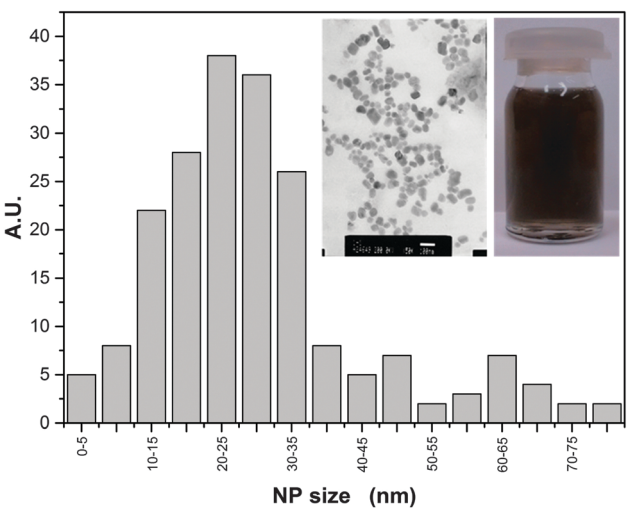

Fig. 1 The size distribution of Ag NPs. Inset shows the view of the Ag dispersion in glycerol (right) and the SEM image (left). The visible arrangement of NPs can be considered as the result of the sample preparation for the SEM visualization.

Open Access Article. Published on 12 June 2015. Downloaded on 12/5/2025 12:04:56 PM.
This article is licensed under a Creative Commons Attribution 3.0 Unported Licence.

measurements the Ag nanocolloid samples were mixed ultrasonically for few hours, to preserve the uniform dispersion of the NPs.

Dynamics of the pressurized glycerol and the Ag–glycerol nanocolloid were tested using the piston-based high pressure set-up, described in ref. 52. The gap of the flat parallel measurement capacitor was equal to 0.2 mm. The macro size of the gap made it possible to reduce parasitic artifacts associated with gas bubbles, finite dimensions or very large intensities of the measurement electric field, which appears for micrometric gaps.

The BDS spectrum was monitored using the Novocontrol BDS Alpha spectrometer giving permanent six number resolution for imaginary and real parts of the dielectric permittivity. This paper focuses on the pressure evolution of DC conductivity σ and the primary relaxation time τ_α. The latter was estimated directly from the peak frequency of the dielectric loss curves from $\tau_\alpha = 1/2\pi f_{peak} = 1/\omega_{peak}$. The DC conductivity from the low frequency increased by the dependence: $\varepsilon''(f) = \sigma/\varepsilon_0\omega$.[2,12] Typical BDS spectra obtained and analyzed in this research were characteristic both for temperature and pressure studies, and are shown in Fig. 2.

It is worth stressing that the BDS offers unique possibilities of high resolution studies both *versus* temperature at atmospheric pressure and under high hydrostatic pressures. Furthermore, the fact that both $\sigma(T,P)$ and $\tau(T,P)$ data can be determined from the same $\varepsilon''(f)$ scan notably reduces biased results and artifacts. So far, BDS studies under high pressures are limited to frequencies: $f < 1 = 10$ MHz, and this is because of still unresolved technical problems.[13] Nevertheless this frequency/time domain clearly correlates with the range of the ultraviscous/ultraslowing domain in the glass forming systems. There is broad evidence from BDS studies under atmospheric pressure focused on FDSE eqn (3) and (9),[2,13,16–41] but surprisingly there are still no results for glycerol, which is one of the accepted glass forming liquids. This can be associated with the fact that glycerol can be encountered as, so called, strong glass formers, for which the clear manifestation of the SB behavior needs to be studied at pressures well above the moderate range of pressures used so far.

This paper presents the results of the first ever FDSE focused test entering the multi GPa domain. High pressure BDS studies were carried out using the innovative piston-based method for the $T \approx 258$ K isotherm, which is well below the room temperature tests that have dominated so far.[17–24] For the selected isotherm the 'glass pressure' can be estimated as $P_g = 1.95$ GPa, using the $T_g(P_g)$ diagram presented in ref. 53. The precision of pressure estimation was equal to 1 MPa and 0.02 K for temperature. All the results were reversible, *i.e.*, they could be obtained both on cooling and heating as well as after compression and decompression. It is notable that earlier FDSE pressure studies were limited to very fragile (strongly SB) glass formers for which applied (moderate) pressures were able to induce significant changes of the timescale.[2,10–26,30,39] For the results presented next, a similar timescale was also obtained for glycerol, because of the extension of the range of pressures, to challenge 1.5 GPa. There have been no reports regarding FDSE behavior in nanocolloids/nanocomposites up to this time.

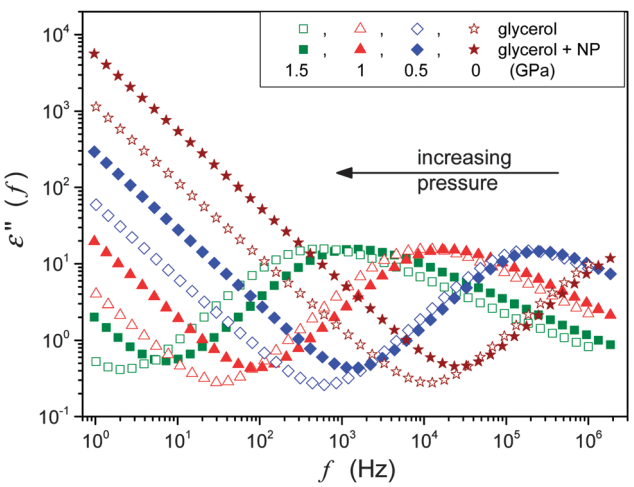

Fig. 2 The behavior of the imaginary part of the dielectric permittivity in glycerol and glycerol + Ag NP nanocolloid. Notable is the increasing impact of Ag NPs on compression.

Results and discussion

This paper focuses on the FDSE behavior in the nanocolloid composed of glycerol and Ag NPs. The 'background' behavior in ultraviscous glycerol, which has been lacked so far, is also discussed.

Fig. 3 shows the pressure evolution of primary relaxation times and DC electric conductivity in glycerol and its nanocolloid with Ag NPs under compression, and the results are in agreement with those of Fig. 2. The addition of NPs notably increases electric conductivity (Fig. 3a, ~decade) and decreases the primary relaxation time (Fig. 3b, ~half a decade). The same pattern is also obtained for the temperature behavior under atmospheric pressure.

The large enhancement in the thermal conductivity and electric conductivity when even a small amount of metallic and other nanoparticles is dispersed is well evidence for lots of systems.[54–58] These extraordinary features have led to a set of innovative applications and to the emergence of a fluid for which there is potentially a large area of practical applications and a new area of research called 'nanofluidics'.[59] Several efforts have been made to explain conductivity enhancements in fluids because of the addition of NPs. However, there has been no general consensus on this issue despite their practical significance.[56–59] No ultimate theoretical model is available to predict nanofluid viscosity with good accuracy.[58,59] Generally, the addition of NPs increases the viscosity of the resulting nanofluid, which is linked to the aggregation of the NPs.[59] However, in viscous heavy oils adding NPs can notably reduce the viscosity.[60–62] This unique behavior is indicated as being particularly important for the petroleum industry.[60] Following eqn (4) and (6) the same pattern may be expected for viscosity

 This journal is © The Royal Society of Chemistry 2015

Open Access Article. Published on 12 June 2015. Downloaded on 12/5/2025 12:04:56 PM.
This article is licensed under a Creative Commons Attribution 3.0 Unported Licence.

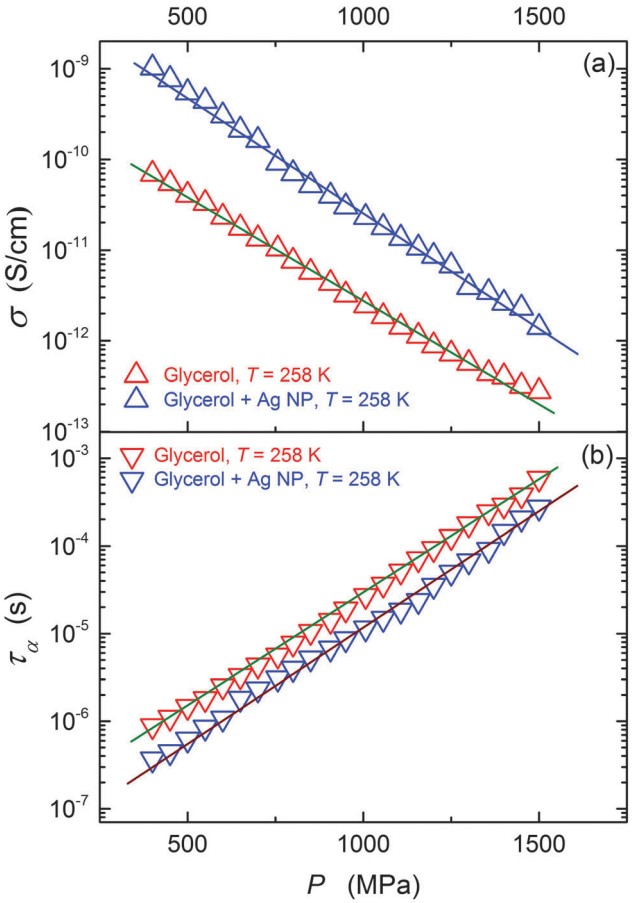

Fig. 3 The pressure evolution of the primary relaxation time (τ) and DC conductivity (σ) for pure glycerol and glycerol + Ag NP composite.

and primary relaxation time. For the latter, the direct experimental evidence is very poor. Nevertheless, for a few 'dense' fluid systems the atypical increase of electric conductivity matching the decrease of the primary relaxation time have been reported.[61–64] This paper presents the first ever results for an ultraviscous glass forming nanocolloid/nanofluid, supercooled and superpressed.

Generally, in very viscous and ultraviscous systems the self-aggregation of the NPs can be difficult and the ultrasonication can further support the stable and homogeneous dispersion of the NPs. Consequently, the self-aggregation most often observed in 'typical' nanofluids can be limited or even avoided. The behavior of the ultraviscous liquids near the T_g is dominated by the emergence of 'dynamic heterogeneities' with a larger density than the fluid-like surrounding and even possible elements of the structural arrangements.[2] This can cause the collection of NPs on the border of solid-like heterogeneities and the fluid-like surroundings and subsequently the fragmentation of the 'heterogeneities'. Consequently, a smaller number of molecules is located within the heterogeneities which can lead to a decrease of the average rotational relaxation time and can also support the decrease of the viscosity. The hypothetical string-like arrangements of the DHs in the ultraviscous domain near the T_g[2] can facilitate string-like arrangements of NPs.

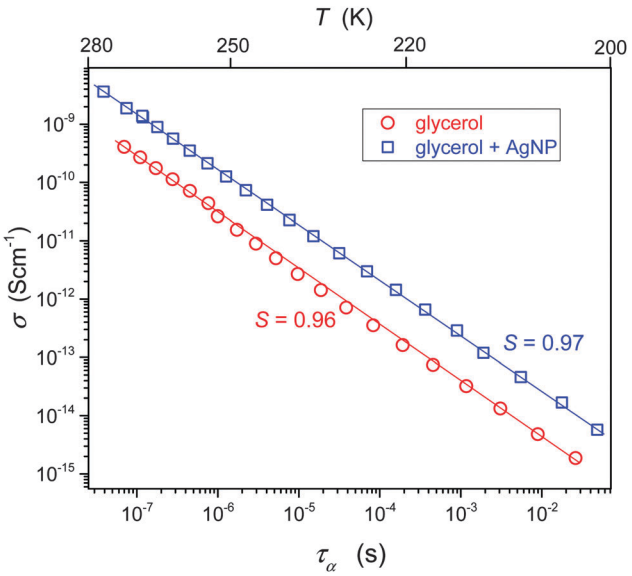

Fig. 4 Temperature test of the DSE law in pure glycerol and glycerol + Ag NP composite at the pressure P = 0.1 MPa. The right scale is for the nanocolloid and the left one for glycerol. Slopes of lines, used to determine the FDSE exponent, are also given.

Such behavior can support larger electric and heat conductivity. The decrease of viscosity can also be supported by the appearance of string-like, elongated mesoscale structures in a similar way as in the addition of a selected polymer to a fluid. It is notable that the increase of electrical conductivity matched the decrease of the relaxation time and viscosity and was observed in NP doped liquid crystals,[63,64] in which the behavior was dominated by multimolecular, pretransitional fluctuations.[65]

Fig. 4 shows the interplay between the translational and orientational dynamics in pure and Ag NP doped glycerol. The analysis shows that in glycerol for $T_B < T < T_g$ the FDSE exponent $S \approx 1$. Thus, in glycerol alone, a negligible decoupling between the DC conductivity and the relaxation time takes place. This behavior is atypical, when comparing it with the

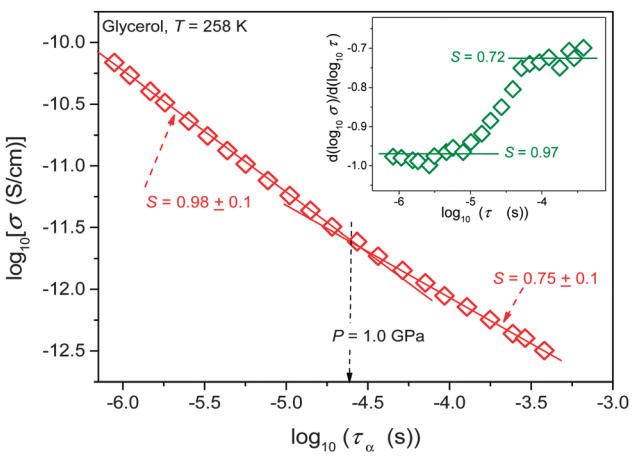

Fig. 5 Test of the fractional DSE behavior in pressurized glycerol at T = 258 K. The inset shows results of the derivative-based, distortion sensitive analysis of the data taken from the main part of the plot.

Open Access Article. Published on 12 June 2015. Downloaded on 12/5/2025 12:04:56 PM.
This article is licensed under a Creative Commons Attribution 3.0 Unported Licence.

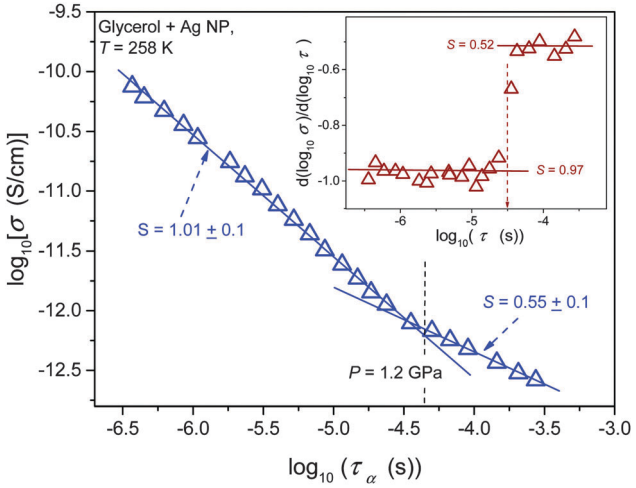

Fig. 6 Test of the fractional DSE behavior in pressurized nanocolloid (glycerol + Ag NPs) at T = 258 K. The inset shows the results of the derivative-based, distortion sensitive analysis of data from the main part of the plot.

dominating evidence for other glass forming liquids, indicating that $S < 1$ for the ultraviscous region.

Results of the analysis of the translational–orientational decoupling on compressing up to P = 1.5 GPa are presented in Fig. 5 for glycerol and in Fig. 6 for the nanocolloid. For glycerol up to $P \sim 1$ GPa the FDSE exponent $S \approx 1$, *i.e.*, the behavior resembles the behavior observed under atmospheric pressure. However, on further pressurization towards the glass transition the gradual translational–orientational decoupling towards the exponent $S \approx 0.75$ occurs. For glycerol plus Ag NP nanocolloid this transformation is 'sharp' and occurs at a well-defined pressure $P \approx 1.2$ GPa, where a jump from $S \approx 1$ to an extremely decoupled FDSE behavior at $S \approx 0.5$ takes place.

The FDSE behavior observed under pressure can be correlated with the broadening of the primary relaxation loss curves, as shown in Fig. 7. Up to $P \approx 1$ GPa, a clear superposition of loss curves takes place. For higher pressures the broadening, both for the high- and low-frequency branches of loss curves, also occurs.

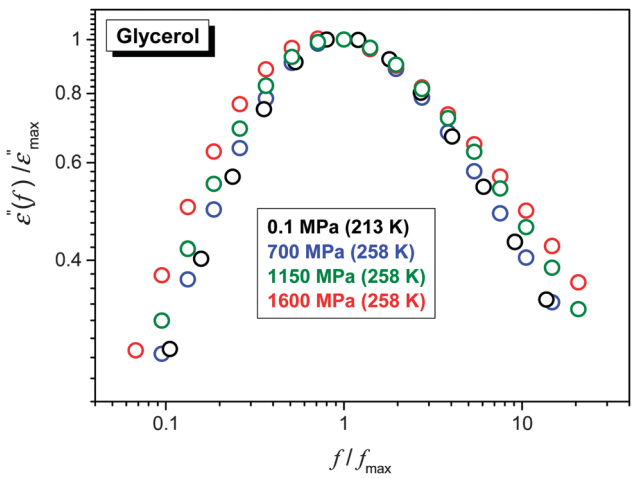

Fig. 7 Normalized superposition of dielectric loss curves $\varepsilon''(f)$ for ultraviscous glycerol under various pressures.

The comparison of $\varepsilon''(f)$ evolution in Fig. 2 and 7 enables a qualitative explanation of FDSE coupling/decoupling manifested by eqn (4) and (13). In Fig. 1 the primary relaxation time is determined from coordinates of the loss curve peak as $\tau = 1/\omega_m = 1/2\pi f_{peak}$ and the DC electric conductivity is using the plot: $y = \log_{10}\varepsilon''(\log_{10}f) = ax + b = a(\log_{10}f) + b$ with the slope $a = 1$, from the linear behavior in the low frequency part of the spectrum. If the low frequency branch of $\varepsilon''(f)$ loss curves do not change, the shift of $\sigma(T,P)$ exactly follows the shift of $\tau(T,P)$ on cooling or pressurization. However, the broadening of $\varepsilon''(f)$ on cooling or pressuring the loss curve induces an extra shift of $\sigma(f)$, which can result in FDSE decoupling by eqn (13).

Conclusions

Glycerol is a versatile material because of its enormous significance in a variety of applications ranging from biotechnology to pharmaceuticals, cosmetics, 'green and biodegradable' plastics, textiles and foodstuffs.[66–69] Glycerol and Ag NP based nanocolloids/nanocomposites are important in these applications because of the well-known antimicrobial activity of Ag NPs.[70,71]

From the fundamental point of view, glycerol has a simple molecular structure, large permanent dipole moment and a relatively small electric conductivity, which coincides with the preferred features for the BDS monitoring.[12] It can be also very easily supercooled. All these reasons mean that glycerol is used as a model 'classical' system in glass transition studies.[2,12,13] This paper also presents the first ever experimental report of FDSE behavior in a nanocolloid–nanocomposite system. Also the range of high pressure implemented is considerably higher than that used in earlier studies. The key result of the paper is the crossover from the almost coupled (DSE) to the strongly decoupled (FDSE) behavior for the pressurized glycerol and glycerol-based nanocolloid in the vicinity of the glass transition. For the extremely decoupled state associated with $S \approx 0.5$, which is probably the lowest value of the FDSE exponent detected so far, the crossover takes place within the non-ergodic ultraviscous domain where so far it was observed solely for the transition into the ultraviscous domain (ergodic–non-ergodic transformation) at much larger distances from the glass transition. The crossover within the pressurized ultraviscous domain takes place both for the 'pure' pure glycerol ($S \approx 1 \rightarrow S \approx 0.7$) and glycerol + Ag NP nanocolloid ($S \approx 1 \rightarrow S \approx 0.5$). For the latter it took place for one, well-defined pressure. Thus, the presence of NPs leads to a qualitative enhancement of manifestations of this phenomenon. The explanation of origin of this phenomenon needs further experimental studies to follow the NPs in the immediate vicinity of the glass transition under high pressure, which in fact is beyond the current experimental state-of-the-art. New possibilities can be opened using advanced microscopic observations

 This journal is © The Royal Society of Chemistry 2015

Open Access Article. Published on 12 June 2015. Downloaded on 12/5/2025 12:04:56 PM.
This article is licensed under a Creative Commons Attribution 3.0 Unported Licence.

of highly compressed liquids, based on the set-up currently built in the lab of the authors. One speculative explanation can be related to better definition of heterogeneities because of the inclusion of NPs. Their possible chain-like arrangements can create elements of uniaxial, orientational ordering within heterogeneities. As shown recently, the fragility is proportional to the parameter n describing the local, symmetry $m \propto n$, with $0.2 < n < 1.5$: the lower value is for the dominated positional ordering, the upper limit is for the clearly orientated case and $n = 1$ is for the 'no-symmetry' case. It is also seen that pressurization notably increases density (for glycerol in the GPa domain down to 20%), thus decreasing the inter-particle distances which can facilitate the ordering of the Ag NPs. It is also worth recalling Fig. 7 and the discussion nearby which indicates the link of the decrease of the FDSE exponent near the glass temperature to the broadening of the distribution of the primary relaxation time, which is strongly linked to the enhancement of the appearance of the dynamic heterogeneities.

It is noteworthy that the analysis based on $D(T)$, $\eta(T)$ and experimental data indicated for glycerol FDSE exponent $\zeta \approx 0.85$ (eqn (4)),[8] the value suggested as universal ones for the ultraviscous domain. The results in this paper do not confirm this finding. It has been found that glycerol exhibits a unique behavior: (i) first, there is no change of FDSE exponent when passing the dynamic crossover point, namely $S \approx 1$ both below and above (T_B,P_B), (ii) a new (not observed so far) crossover to the behavior governed by $S < 1$ occurs already within the ultraviscous domain, particularly under high compression and (iii) the presence of Ag NPs in the glycerol notably strengthens the features related to the FDSE domain emerging in the immediate vicinity of the glass transition.

The simple analysis based solely on SA and SB relationships and the general FDSE dependences yielded a new link between the FDSE exponent S and temperature and pressure related fragilities indicating that for the $m_T^\sigma = Sm_T^\tau$ and $m_P^\sigma = Sm_P^\tau$. The larger fragility coefficient for primary relaxation time related processes are in agreement with the above fundamental findings discussed by Sokolov and Schweitzer.[43] Worth stressing is the link obtained of the FDSE exponent to the apparent activation enthalpy and volume.

In conclusion, this report shows new features of translational–orientational decoupling dynamics emerging from the impact of very high pressures on ultraviscous glycerol and the formation of an Ag NP based nanocolloid. The report also indicates that some basic features of the decoupling can be deduced from the general SA, SB and FDSE equations.

Acknowledgements

Research by SJR was carried out with the support of the National Science Centre (Poland) grant No. 2011/01/B/NZ9/02537. The research by ADR and SSz was supported by the National Centre for Science (Poland), grant No. UMO 2011/03/B/ST3/02352.

References

1 D. Kennedy, *Science*, 2005, **309**, 83.
2 K. L. Ngai, *Relaxation and Diffusion in Complex Systems*, Springer, Berlin, 2011.
3 R. A. L. Jones, *Soft Condensed Matter Physics*, Oxford Univ. Press, Oxford, 2002.
4 C. A. Angell, Strong and fragile liquids, in *Relaxations in Complex Systems*, ed. K. L. Ngai and G. B. Wright, National Technical Information Service, U.S. Dept. of Commerce, Springfield, 1985.
5 J. C. Martinez-Garcia, S. J. Rzoska, A. Drozd-Rzoska, S. Starzonek and J. C. Mauro, *Sci. Rep.*, 2015, **5**, 8314.
6 A. L. Agapov, V. N. Novikov and A. P. Sokolov, in *Fragility and other properties of glass-forming liquids: two decades of puzzling correlations*, Fragility of glass forming liquids, ed. L. A. Greer, K. F. Kelton and S. Sastry, Hindustan Book Agency, 2013.
7 A. I. Nielsen, S. Pawlus, M. Paluch and J. C. Dyre, *Philos. Mag.*, 2008, **88**, 4101–4108.
8 F. Mallamace, C. Branca, C. Corsaro, N. Leone, J. N. Spooren, S.-H. Chen and H. E. Stanley, *Proc. Natl. Acad. Sci. U. S. A.*, 2010, **28**, 22457–22462.
9 M. A. Anisimov, *Critical Phenomena in Liquids and Liquid Crystals*, Gordon and Breach, Reading, 1992.
10 V. N. Novikov and A. P. Sokolov, *Phys. Rev. E: Stat., Nonlinear, Soft Matter Phys.*, 2003, **67**, 031507.
11 P. J. Griffin, J. R. Sangoro, Y. Wang, A. P. Holt, V. N. Novikov, A. P. Sokolov, M. Paluch and F. Kremer, *Soft Matter*, 2013, **43**, 10373–10380.
12 F. Kremer and A. Schoenhals, *Broadband Dielectric Spectroscopy*, Springer Verlag, Berlin, 2003.
13 G. Floudas, M. Paluch, A. Grzybowski and K. L. Ngai, *Molecular Dynamics of Glass-Forming Systems: Effects of Pressure*, Springer, Berlin, 2012.
14 K. A. Dill and S. Bromber, *Molecular Driving Forces: Statistical Thermodynamics in Chemistry and Biology*, Garland Science, London, 2011.
15 J. C. Dyre, *Rev. Mod. Phys.*, 2006, **78**, 953–972.
16 L. Andreozzi, A. Di Schino, M. Giordano and D. Leporini, *Europhys. Lett.*, 1997, **38**, 669–674.
17 S. Corezzi, M. Lucchesi and P. A. Rolla, *Philos. Mag. B*, 1999, **79**, 1953–1963.
18 S. Hensel Bielowka, T. Psurek, J. Ziolo and M. Paluch, *Phys. Rev. E: Stat., Nonlinear, Soft Matter Phys.*, 2001, **63**, 062301.
19 P. G. Debenedetti, T. M. Truskett and C. P. Lewis and F. H. Stillinger, Theory of supercooled liquids and glasses. Energy Landscape and Statistical Geometry Perspective, *Advances in Chemical Engineering*, Academy Press, Princeton, 2001, vol. 28, pp. 21–30.
20 M. Paluch, T. Psurek and C. M. Roland, *J. Phys.: Condens. Matter*, 2002, **14**, 9489–9494.
21 M. Paluch, C. M. Roland, J. Gapinski and A. Patkowski, *J. Chem. Phys.*, 2003, **118**, 3177–3186.
22 R. Casalini and C. M. Roland, *J. Chem. Phys.*, 2003, **119**, 4052–4059.

Open Access Article. Published on 12 June 2015. Downloaded on 12/5/2025 12:04:56 PM.
This article is licensed under a Creative Commons Attribution 3.0 Unported Licence.

23 R. Casalini, M. Paluch, T. Psurek and C. M. Roland, *J. Mol. Liq.*, 2004, **111**, 53–60.
24 T. Psurek, J. Ziolo and M. Paluch, *Physica A*, 2004, **331**, 353–364.
25 G. P. Johari and O. Andersson, *J. Chem. Phys.*, 2006, **125**, 124501.
26 O. Andersson, G. P. Johari and R. M. Shanker, *J. Pharm. Sci.*, 2006, **95**, 2406–2418.
27 R. Richertand and K. Samwer, *New J. Phys.*, 2007, **9**, 36.
28 G. Power, J. K. Vij and G. P. Johari, *J. Phys. Chem. B*, 2007, **111**, 11201–11208.
29 M. G. Mazza, N. Giovambattistam, H. E. Stanley and F. W. Starr, *Phys. Rev. E: Stat., Nonlinear, Soft Matter Phys.*, 2007, **76**, 031203.
30 S. Pawlus, M. Paluch, J. Ziolo and C. M. Roland, *J. Phys.: Condens. Matter*, 2009, **21**, 332101.
31 L. Xu, F. Mallamace, Z. Yan, F. W. Starr, S. V. Buldyrev and H. E. Stanley, *Nat. Phys.*, 2009, **5**, 565–569.
32 A. Drozd-Rzoska and S. J. Rzoska, Anomalous Decoupling of the dc Conductivity and the Structural Relaxation Time in the Isotropic Phase of a Rod-like Liquid Crystalline Compound, in *Metastable Systems under Pressure*, ed. S. J. Rzoska, V. Mazur and A. Drozd-Rzoska, Springer, Berlin, 2010, pp. 141–152.
33 G. Sesé, J. O. de Urbina and R. Palomar, *J. Chem. Phys.*, 2012, **137**, 114502.
34 K. V. Edmonda, M. T. Elsesserb, G. L. Huntera, D. J. Pinebo and E. R. Weeksa, *Proc. Natl. Acad. Sci. U. S. A.*, 2012, **109**, 17891–17896.
35 F. Mallamace, C. Corsaro, N. Leone, V. Villari, N. Micali and S.-H. Chen, *Sci. Rep.*, 2014, **4**, 3747.
36 Z. Shi, P. G. Debenedetti and F. H. Stillinger, *J. Chem. Phys.*, 2013, **138**, 12526.
37 N. Leone, V. Villari, N. Micali and S.-H. Chen, *Sci. Rep.*, 2013, **4**, 3747.
38 J. Swiergiel and J. Jadzyn, *Phys. Chem. Chem. Phys.*, 2011, **13**, 3911–3916.
39 Z. Wojnarowska, Y. Wang, J. Pionteck, K. Grzybowska, A. P. Sokolov and M. Paluch, *Phys. Rev. Lett.*, 2013, **111**, 225703.
40 E. Herold, M. Strauch, D. Michalik, A. Appelhagenand and R. Ludwig, *Phys. Chem. Chem. Phys.*, 2014, **15**, 3040–3048.
41 D. A. Turton and K. Wynne, *J. Phys. Chem. B*, 2014, **118**, 4600–4605.
42 *Soft Matter under Exogenic Impacts*, ed. S. J. Rzoska and V. Mazur, Springer, Berlin, 2007.
43 A. P. Sokolov and K. S. Schweitzer, *Phys. Rev. Lett.*, 2009, **102**, 23831.
44 C. Barus, *Proc. Am. Acad. Arts Sci.*, 1891, **27**, 13–15.
45 A. Drozd-Rzoska and S. J. Rzoska, *Phys. Rev. E: Stat., Nonlinear, Soft Matter Phys.*, 2006, **73**, 041502.
46 J. C. Martinez-Garcia, S. J. Rzoska, A. Drozd-Rzoska and J. Martinez-Garcia, *Nat. Commun.*, 2013, **4**, 1823.
47 J. C. Martinez-Garcia, S. J. Rzoska, A. Drozd-Rzoska, J. Martinez-Garcia and J. C. Mauro, *Sci. Rep.*, 2014, **4**, 5160.
48 M. Paluch, S. J. Rzoska and J. Zioło, *J. Phys.: Condens. Matter*, 1998, **10**, 4131–4138.
49 A. Drozd-Rzoska, S. J. Rzoska and C. M. Roland, *J. Phys.: Condens. Matter*, 2008, **20**, 244103.
50 L. Barber and T. Kistersky, *Apparatus and method for localized ion sputtering/Publ*, *US Pat.*, 5591313, 1997.
51 P. Liu, Y. Liang, H. B. Li and G. W. Yang, *Nanomaterials: Applications and Properties*, NAP, Beijing, 2011, vol. 1, pp. 136–150.
52 M. Paluch, M. Sekula, S. Pawlus, S. J. Rzoska, J. Ziolo and C. M. Roland, *Phys. Rev. Lett.*, 2003, **90**, 175702.
53 A. Drozd-Rzoska, S. J. Rzoska, M. Paluch, A. R. Imre and C. M. Roland, *J. Chem. Phys.*, 2007, **126**, 164504.
54 S. U. S. Choi, Z. G. Zhang, W. Yu, F. E. Lockwood and E. A. Grulke, *Appl. Phys. Lett.*, 2001, **79**, 2252–2254.
55 J. A. Eastman, S. U. S. Choi, S. Li, W. Yu and W. Thompson, *Appl. Phys. Lett.*, 2001, **78**, 718.
56 P. Warrier and A. Teja, *Nanoscale Res. Lett.*, 2011, **6**, 247–253.
57 I. M. Mahbubul, R. Saidur and M. A. Amalina, *Int. J. Heat Mass Transfer*, 2012, **55**, 874–888.
58 S. B. White, A. Jau-Min Shih and K. P. Pipe, *Nanoscale Res. Lett.*, 2011, **6**, 346.
59 S. K. Das, S. U. Choi, W. Yu and T. Pradeep, *Nanofluids: Science and Technology*, Wiley, NY, 2008.
60 Y. H. Shokrlu and T. Babadagli, *J. Pet. Sci. Eng.*, 2014, **119**, 210–220.
61 R. J. Sengwa, S. Choudhary and S. Sankhla, *eXPRESS Polym. Lett.*, 2008, **2**, 800–809.
62 M. Dong, L. P. Shen, H. Wang, H. B. Wang and J. Miao, *J. Nanomater.*, 2013, **2013**, 1–7.
63 S. P. Yadav, M. Pande, R. Manohan and S. Singh, *J. Mol. Liq.*, 2015, **208**, 34–37.
64 S. Krishna Prasad, M. Vijay Kumar, T. Shilpa and C. V. Yelamaggad, *RSC Adv.*, 2014, **4**, 4453–4462.
65 S. J. Rzoska, A. Drozd-Rzoska, P. K. Mukherjee, D. O. Lopez and J. C. Martinez-Garcia, *J. Phys.: Condens. Matter*, 2013, **25**, 245105.
66 M. Pagliaro and M. Rossi, *Future of Glycerol: New Usages for a Versatile Raw Material*, RSC, Cambridge, 2008.
67 E. S. Stevens, *Green Plastics: An Introduction to the New Science of Biodegradable Plastics*, Princeton Univ. Press, Princeton, 2002.
68 F. Gunstone, *Oils and Fats in the Food Industry*, Wiley & Sons, NY, 2009.
69 J. Choi and J. C. Bishof, *Cryobiology*, 2010, **60**, 49–52.
70 C. Balny and R. Hayashi, *High Pressure Bioscience and Biotechnology*, Progress in Biotechnology, Elsevier, Amsterdam, vol. 13, 1996.
71 J. A. Lemire, J. J. Harrison and R. J. Turner, *Nat. Rev. Microbiol.*, 2013, **11**, 371–384.

This journal is © The Royal Society of Chemistry 2015